Title

All-optical switching of nematic liquid crystal films driven by localized surface plasmons

Journal

Optics Express, 23(5)

ISSN

1094-4087

Authors

Quint, Makiko T

Delgado, Silverio

Paredes, John H

et al.

Publication Date

2015-03-09

DOI

10.1364/oe.23.006888

Peer reviewed

All-optical switching of nematic liquid crystal films driven by localized surface plasmons

Makiko T. Quint,[1] Silverio Delgado,[1] John. H. Paredes,[2] Zachary S. Nuno,[1] Linda S. Hirst,[1,2] and Sayantani Ghosh[1,*]

[1]*Department of Physics, School of Natural Sciences, University of California, Merced, California 95343, USA*
[2]*School of Engineering, University of California, Merced, California 95343, USA*
[2]*lhirst@ucmerced.edu*
[*]*sghosh@ucmerced.edu*

Abstract: We have demonstrated an all-optical technique for reversible in-plane and out-of-plane switching of nematic liquid crystal molecules in few micron thick films. Our method leverages the highly localized electric fields ("hot spots") and plasmonic heating that are generated in the near-field region of densely packed gold nanoparticle layers optically excited on-resonance with the localized surface plasmon absorption. Using polarized microscopy and transmission measurements, we observe this switching from homeotropic to planar over a temperature range starting at room temperature to just below the isotropic transition, and at on-resonance excitation intensity less than 0.03 W/cm^2. In addition, we controllably vary the in-plane directionality of the liquid crystal molecules in the planar state by altering the linear polarization of the incident excitation. Using discrete dipole simulations and control measurements, we establish spectral selectivity in this new and interesting perspective for photonic application using low light power.

OCIS codes: (230.1150) All-optical devices; (230.3720) Liquid-crystal devices; (250.5403) Plasmonics; (250.6715) Switching.

References and links

1. A. Choudhary, G. Singh, and A. M. Biradar, "Advances in gold nanoparticle-liquid crystal composites," Nanoscale **6**(14), 7743–7756 (2014).
2. R. Bitar, G. Agez, and M. Mitov, "Cholesteric liquid crystal self-organization of gold nanoparticles," Soft Matter **7**(18), 8198–8206 (2011).
3. S. Kumar, S. K. Pal, P. S. Kumar, and V. Lakshminarayanan, "Novel conducting nanocomposites: synthesis of triphenylene-covered gold nanoparticles and their insertion into a columnar matrix," Soft Matter **3**(7), 896–900 (2007).
4. H. Qi, B. Kinkead, V. M. Marx, H. R. Zhang, and T. Hegmann, "Miscibility and Alignment Effects of Mixed Monolayer Cyanobiphenyl Liquid-Crystal-Capped Gold Nanoparticles in Nematic Cyanobiphenyl Liquid Crystal Hosts," ChemPhysChem **10**(8), 1211–1218 (2009).
5. A. Demortière, S. Buathong, B. P. Pichon, P. Panissod, D. Guillon, S. Bégin-Colin, and B. Donnio, "Nematic-like Organization of Magnetic Mesogen-Hybridized Nanoparticles," Small **6**(12), 1341–1346 (2010).
6. Y. K. Verma, R. H. Inman, C. G. L. Ferri, H. Mirafzal, S. N. Ghosh, D. F. Kelley, L. S. Hirst, S. Ghosh, and W. C. Chin, "Electrical modulation of static and dynamic spectroscopic properties of coupled nanoscale GaSe quantum dot assemblies," Phys. Rev. B **82**(16), 165428 (2010).
7. X. Zeng, F. Liu, A. G. Fowler, G. Ungar, L. Cseh, G. H. Mehl, and J. E. Macdonald, "3D Ordered Gold Strings by Coating Nanoparticles with Mesogens," Adv. Mater. **21**(17), 1746–1750 (2009).
8. A. Rodarte, R. Pandolfi, S. Ghosh, and L. S. Hirst, "Quantum dot/liquid crystal composite materials: Self-assembly driven by liquid crystal phase transition templating," J. Mater. Chem. C. **1**(35), 5527–5532 (2013).
9. H. Qi and T. Hegmann, "Formation of periodic stripe patterns in nematic liquid crystals doped with functionalized gold nanoparticles," J. Mater. Chem. **16**(43), 4197–4205 (2006).
10. W. Dickson, G. A. Wurtz, P. R. Evans, R. J. Pollard, and A. V. Zayats, "Electronically controlled surface plasmon dispersion and optical transmission through metallic hole arrays using liquid crystal," Nano Lett. **8**(1), 281–286 (2008).

#232186 - $15.00 USD Received 9 Jan 2015; revised 16 Feb 2015; accepted 17 Feb 2015; published 5 Mar 2015

11. P. A. Kossyrev, A. Yin, S. G. Cloutier, D. A. Cardimona, D. Huang, P. M. Alsing, and J. M. Xu, "Electric Field Tuning of Plasmonic Response of Nanodot Array in Liquid Crystal Matrix," Nano Lett. **5**(10), 1978–1981 (2005).
12. O. Buchnev, J. Y. Ou, M. Kaczmarek, N. I. Zheludev, and V. A. Fedotov, "Electro-optical control in a plasmonic metamaterial hybridised with a liquid-crystal cell," Opt. Express **21**(2), 1633–1638 (2013).
13. M. Decker, C. Kremers, A. Minovich, I. Staude, A. E. Miroshnichenko, D. Chigrin, D. N. Neshev, C. Jagadish, and Y. S. Kivshar, "Electro-optical switching by liquid-crystal controlled metasurfaces," Opt. Express **21**(7), 8879–8885 (2013).
14. L. De Sio, G. Klein, S. Serak, N. Tabiryan, A. Cunningham, C. M. Tone, F. Ciuchi, T. Burgi, C. Umeton, and T. Bunning, "All-optical control of localized plasmonic resonance realized by photoalignment of liquid crystals," J. Mater. Chem. C. **1**(45), 7483–7487 (2013).
15. Q. Liu, N. Wang, P. Chen, Y. Zhang, and S. He, "Large-area bulk self-assembly of plasmonic nanorods in nematic liquid crystal via surface mediated Alignment," Opt. Mater. Express **3**(11), 1918–1924 (2013).
16. G. Gilardi, S. Xiao, N. A. Mortensen, A. d'Alessandro, and R. Beccherelli, "Plasmon resonance optical tuning based on photosensitive composite structures," J. Opt. Soc. Am. B **31**(2), 360–365 (2014).
17. Q. Liu, Y. Yuan, and I. I. Smalyukh, "Electrically and Optically Tunable Plasmonic Guest-Host Liquid Crystals with Long-Range Ordered Nanoparticles," Nano Lett. **14**(7), 4071–4077 (2014).
18. S. A. Maier, *Plasmonics: Fundamentals and Applications* (Springer, 2007).
19. S. Nie and S. R. Emory, "Probing Single Molecules and Single Nanoparticles by Surface-Enhanced Raman Scattering," Science **275**(5303), 1102–1106 (1997).
20. P. P. Pompa, L. Martiradonna, A. D. Torre, F. D. Sala, L. Manna, M. De Vittorio, F. Calabi, R. Cingolani, and R. Rinaldi, "Metal-enhanced fluorescence of colloidal nanocrystals with nanoscale control," Nat. Nanotechnol. **1**(2), 126–130 (2006).
21. T. P. Bigioni, X.-M. Lin, T. T. Nguyen, E. I. Corwin, T. A. Witten, and H. M. Jaeger, "Kinetically driven self assembly of highly ordered nanoparticle monolayers," Nat. Mater. **5**(4), 265–270 (2006).
22. J. Smith, J. Faucheaux, S. White, A. N. Sobh, J. Feser, P. K. Jain, and N. Sobh, "nanoDDSCAT," (DOI:10.4231/D3G73746M, (2015). *https://nanohub.org/resources/dda*.
23. M. Oh-e and K. Kondo, "Response mechanism of nematic liquid crystals using the in-plane switching mode," Appl. Phys. Lett. **69**(5), 623–626 (1996).
24. T. Ikeda and O. Tsutsumi, "Optical Switching and Image Storage by Means of Azobenzene Liquid-Crystal Films," Science **268**(5219), 1873–1875 (1995).
25. P. K. Jain, K. S. Lee, I. H. El-Sayed, and M. A. El-Sayed, "Calculated absorption and scattering properties of gold nanoparticles of different size, shape, and composition: applications in biological imaging and biomedicine," J. Phys. Chem. B **110**(14), 7238–7248 (2006).
26. G. Baffou, R. Quidant, and F. J. García de Abajo, "Nanoscale control of optical heating in complex plasmonic systems," ACS Nano **4**(2), 709–716 (2010).

1. Introduction

The synergy between metallic gold nanoparticles (AuNPs) and liquid crystalline (LC) molecules has been widely investigated in the recent years from a variety of perspectives, both topological and functional. The initial studies of NP solubility and dispersion in nematic LC materials were conducted using AuNPs [1–4] and while these have now broadened in scope to include other types of NPs [5, 6], the study of AuNPs in LC continue to unearth exciting phenomena. These include the formation of LC phase transition driven ordered assemblies of AuNPs [7, 8] and stripe formation in nematic LC doped with chiral ligand-capped AuNPs [9]. From a functional perspective, LCs are a particularly compatible and unique host for AuNPs, since the refractive index of the electro-optically active LC host can be controllably altered by many external parameters (such as temperature, light, and electric field) to tune the localized plasmon resonance (LPR) of the AuNPs dispersed within. This aspect has made LCs the ideal materials for designing novel active plasmonic devices that are easily reconfigurable *in situ*, where typically an external electric field is used to drive the LC orientational changes, which, in turn tune the LPR [10–13]. There are additional instances of light-driven tuning of LPR using additional alignment layers LCs [14, 15], dye-LC composite mixtures [16], and of using LC re-orientation to control AuNP directionality [17]. In all these studies, the focus is on altering the spectral properties of the AuNPs by changing the LC orientation. We present results of the radically alternative approach, where the scattered electric field generated on-resonance by an ensemble of AuNPs is used to controllably and reversibly re-orient nematic LC molecules in a few (1 – 2) μm thick LC film.

#232186 - $15.00 USD Received 9 Jan 2015; revised 16 Feb 2015; accepted 17 Feb 2015; published 5 Mar 2015

LPRs are the localized versions of surface plasmon polaritons (SPPs). While SPP are propagating oscillations of the conduction electrons at a metal film-dielectric interface, LPRs are observed in metallic NPs. At specific frequencies of an incident time-varying electric field, NPs exhibit resonantly enhanced scattering and absorption in the near-field regime. The resonance condition is set by a specific relation between the frequency-dependent NP permittivity and the dielectric constant of the surrounding medium, known as Frohlich's condition [18]. In an ensemble of densely packed NPs, in the limit $d \ll \lambda$, where d is the interparticle separation and λ the wavelength of the incident field, the NPs act like interacting dipoles and far-field scattering is strongly suppressed. The result is highly localized scattered fields in the space between the NPs, creating what are popularly known as "hot spots". This phenomenon is widely exploited in well-known optical detention techniques such as SERS (Surface Enhanced Raman Scattering) [19] and MEF (Metal Enhanced Fluorescence) [20]. In this study, we use the highly confined scattered field generated during resonant excitation in the interstitial regions of a densely packed layer of AuNPs to switch directionality of a nematic LC film deposited on top of the gold layer. This re-orientation is reversible and repeatable, and does not require either photo-alignment coatings or any additional applied electric field. We observe this switching over a temperature range starting at room temperature and up to a few degrees below the isotropic transition, and at on-resonance excitation intensity less than 0.03 W/cm^2. In addition, we can controllably switch the in-plane directionality of the LC molecules in the planar state by altering the linear polarization of the incident excitation.

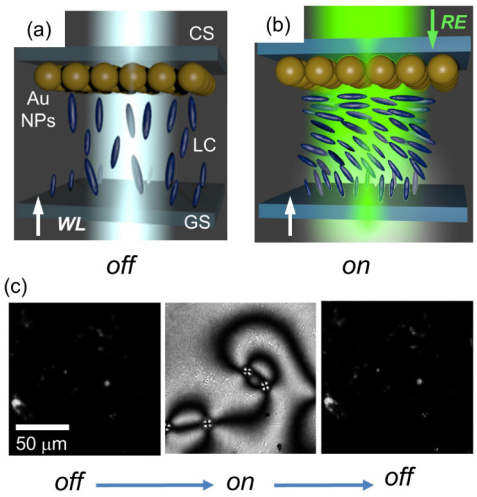

Fig. 1. Schematic of experimental set up demonstrating (a) 'Off' configuration with only white light (WL) beam, and (b) 'On' configuration with WL and resonant excitation (RE) beams. CS: Cover slip; AuNPs: gold nanoparticles; LC: Liquid crystal; GS: glass slide (c) series of polarized microscopy images of LC sample at 30°C starting with resonant beam off, then turned on and then off again.

2. Experimental details

Figure 1(a) shows the structure of a typical sample. A 10 µL droplet of the citrate-ligated 30 nm AuNP solution (Sigma Aldrich) is deposited on a cleaned cover slip (CS). The solvent is allowed to evaporate naturally for 10 h to form an AuNP layer [21], after which 5 µL of nematic LC 4-cyano-4-pentylbiphenyl (5CB, sigma Aldrich) in the isotropic phase is deposited onto a cleaned standard glass slide (GS) and covered with the AuNP layered cover slip. The device is designed to exhibit a homeotropic LC alignment in this arrangement, using clean glass on the upper surface and the citrate ligated AuNPs on the lower surface.

#232186 - $15.00 USD Received 9 Jan 2015; revised 16 Feb 2015; accepted 17 Feb 2015; published 5 Mar 2015

Homeotropic alignment of the device is verified by rotation between crossed polarizers on the optical microscope. Extinction spectra for our samples are taken using a PerkinElmer UV/VIS spectrophotometer. For LC phase imaging we use a Leica DM2500P upright polarized optical microscope (POM). For additional temperature, power and wavelength dependence of the switching effect, we use a custom-designed optical set-up with two excitation sources: a continuous wave diode laser tuned to 532 nm (Verdi V6, Coherent Inc.) and a tunable (700 – 1000 nm) Ti:Sapphire laser (MIRA 900, Coherent inc.). A tungsten halogen lamp (HL-2000, Ocean Optics) is used as the broadband white light (WL) detection source. The excitation and WL beams are focused onto the sample, which is mounted on a heating stage (Instec Inc.) attached to a 3D mechanized scanning stage. Crossed polarizers, half wave-plates and silicon-amplified photodetectors are incorporated in the path for transmission and in-plane rotation measurements.

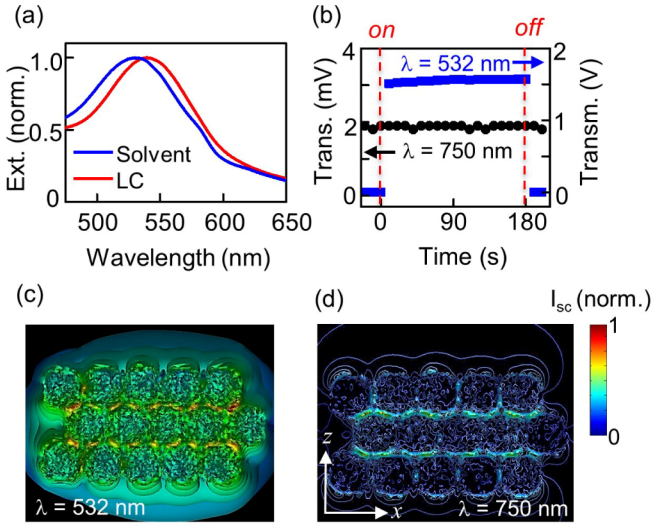

Fig. 2. (a) Extinction spectra of 30 nm AuNPs suspended in its buffer solvent (blue) and in 5CB (red). (b) Transmission of WL as measured by photo-detector for resonant (blue squares) and non-resonant (black circles) excitation. Dashed lines indicate when the excitation light is turned on and off. Near–field simulations of scattered E-field intensity when incident excitation is (c) resonant (532 nm) and (d) non-resonant (750 nm) with the AuNP extinction peak in (a). The incident light is incident along the y-axis and polarized along the z-axis.

3. Results and discussions

The AuNP layer promotes homeotropic surface anchoring and therefore 5CB molecules orient perpendicular to the glass slides as shown in the schematic in Fig. 1(a). Under crossed polarizers in the POM, the transmission image taken at 30°C with only the WL appears dark [Fig. 1(c, left)] and we denote this the 'Off' state. When the sample is illuminated with an additional beam of wavelength in 515-560 nm range, as shown in Fig. 1(b), the transmission of WL is now much higher, and the corresponding image [Fig. 1(c, center)] is bright over large regions, indicating that some of the LC molecules have re-oriented in the plane of the sample (planar alignment). This is designated the 'On' state, where the AuNPs induce a local planar alignment close to the particles.This creates a hybrid device configuration in the case that the upper glass plate is homeotropically aligned. This spectral band is chosen as it is inclusive of the LPR peak for 30 nm AuNP, verified in Fig. 2(a). As soon as the second excitation is turned off, the transmission reverts back to the initial dark image [Fig. 1(c, right)] and the sample is again in the 'Off' state.

#232186 - $15.00 USD Received 9 Jan 2015; revised 16 Feb 2015; accepted 17 Feb 2015; published 5 Mar 2015

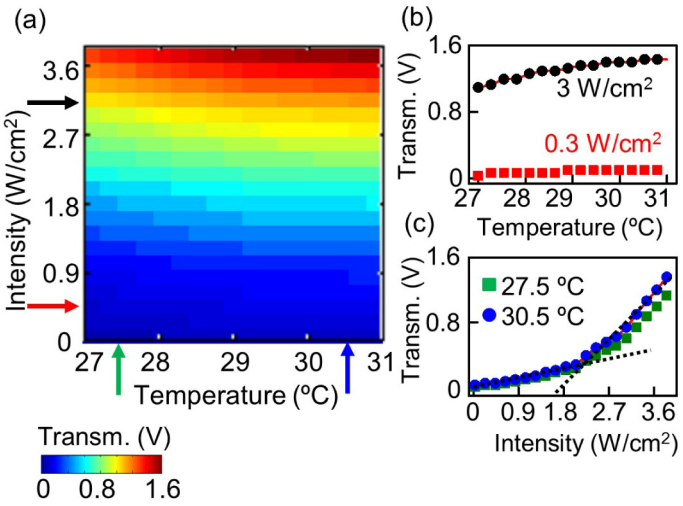

Fig. 3. (a) Transmission in 'on' mode mapped out as functions of resonant excitation intensity and sample temperature. (b) Transmission varying with temperature for two different excitation intensities, derived from line cuts along arrows shown in (a), (c) transmission changing with intensity at two different temperatures. Arrows in (a) show positions of line-cuts. Dashed lines in (c) indicate intensity where linear behaviour is disrupted.

Figure 2(a) compares the extinction (scattering and absorption) spectra of our AuNPs when suspended in the citrate buffer (blue) and in 5CB (red). The latter shows a slight red-shift, as is expected due to the LC's higher dielectric constant. Figure 2(b) is a plot of the variation of WL transmission voltage with time, as measured by a photo-detector when excitations are turned on and off (dashed lines). For excitation with 0.03 W/cm^2 of λ = 532 nm light, the transmission shows a clear increase at 'on' followed by a return to almost zero at 'off'. In the duration of the 'on' period, the transmission remains almost flat, indicating the stability of the state. We have increased this time period up to 30 min and not observed any instability. The same protocol using λ = 750 nm excitation is also shown for comparison. Figure 2(c) is a simulation of a small array of 15 30 nm diameter AuNPs arranged in hexagonal close-packed arrangement typical of densely packed nanoparticle films formed by dropcast method [21]. The near-field scattering pattern, simulated using discrete dipole approximation (DDSCAT) [22] and shows the developments of "hot-spots" when illuminated with wavelength λ = 532 nm. The ***E***-field enhancement factors at these spots in between 10 and 50. By comparison, scattering is strongly suppressed when this ensemble is excited with λ = 750 nm light [Fig. 2(d)] at the same average power. While these simulations use simplified arrangements of the AuNPs, they complement the observations of Fig. 2(b). Establishing the wavelength selectivity of LC re-orientation is an important component as it confirms that the origin of the observed switching is not associated with bulk heating of the LC film by the pump lasers for the excitation powers used.

In Fig. 3(a) we map the on-resonance transmission in the "on" state as a function of excitation intensity and sample temperature. Temperature is varied from 27° C to 31° C, to ensure 5CB is in the nematic state (N – I transition occurs at 35° C) and excitation intensity is varied from 0.03 – 4.31 W/cm^2 at each temperature. Line cuts along fixed intensity in Fig. 3(b) confirms that at low powers, transmission is temperature independent. At higher intensities there is an increase in transmission by ~28% over the measured temperature range. Similar data at 27.5° C and 30.5° C in Fig. 3(c) show that the intensity dependence of transmission demonstrates linear behavior up to ~2 W/cm^2, followed by a steep three-fold increase at higher powers for both temperatures. This indicates that incident intensity greater than 2 W/cm^2 cause some perturbations, most likely associated with localized heating.

#232186 - $15.00 USD Received 9 Jan 2015; revised 16 Feb 2015; accepted 17 Feb 2015; published 5 Mar 2015

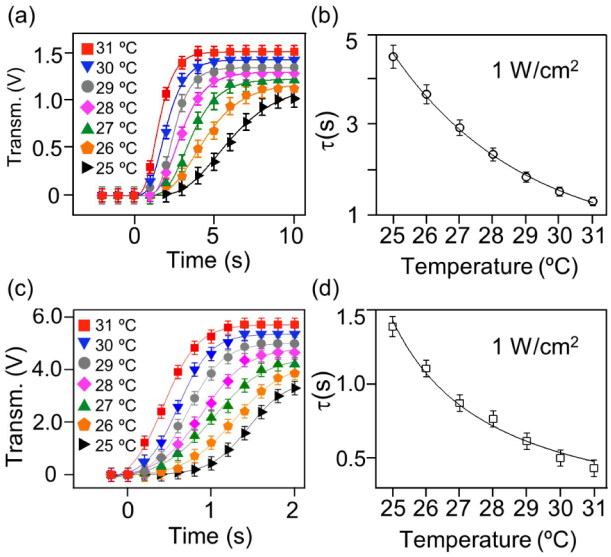

Fig. 4. Transmission measured as a function of time. The AuNPs are drop casted on (a) only the cover slip and (c) both the cover slip and the glass slide. The rise times at different temperatures for (b) a cover slip and (d) both a cover slip and glass slide samples. Time = 0 s denotes when resonant excitation is switched on.

Figure 4(a) shows the transmission sharply increases when the 532 nm excitation is switched on at '0' s. Fits to data allow us to determine τ, plotted in Fig. 4(b). While typical switching times for nematic LCs are on the order of milliseconds [23, 24], our samples exhibit longer times, between 1.5 – 3 s. This slow response is not entirely unexpected, given the geometry of our samples, where there is a large contrast between the thicknesses of the AuNP layer and the LC film. The AuNPs typically form a monolayer, though AFM measurements have shown occasional formation of up to four multilayers in certain regions, which account for the orientational non-uniformity observed in Fig. 1(c). The plasmonic field generated by these AuNPs falls of exponentially over a depth of few tens of nm, which means only a few layers of LC molecules are under the direct influence of the scattered electric field. The time τ we measure and plot in Fig. 4(b) is therefore the time for the elastic deformation of those few LC molecules to propagate through the remaining 1-2 μm thick LC film. The decrease in response time with increasing excitation power can be attributed to localized plasmonic heating. When excited on-resonance the AuNPs can generate thermal gradients that, while strongly localized, scales with the incident power and can therefore be substantial [25]. We estimate the maximum temperature change following formulation in ref [26]. for our highest excitation intensity (4 W/cm^2) to be ~0.1°C. This formulation is approximate, and our densely packed film possibly develops larger thermal gradients. Increasing thermal fluctuations in the nematic phase will decrease both Frank elastic constants and the viscosity of the nematic phase, particularly when the material is close to the clearing point where such fluctuations are significant. In addition, thermal fluctuations are expected to weaken anchoring conditions at the particle surface and this effect may also reduce both the threshold field for switching and the response time. To put this to test, we re-designed our samples with AuNP layers deposited on both top and bottom surfaces, and the transmission data is shown in Fig. 4(c). Not only is the total transmission higher than in Fig. 4(a), the time scales are reduced as well, ranging from 1.5 – 0.5 s as shown in Fig. 4(d). This is an encouraging trend, and these response times can be further improved by the use of thinner LC films, different LC materials optimized for display applications and AuNPs with morphologies tailored for plasmonic applications, such as nanorods, nanoprisms and bow-tie structures.

#232186 - $15.00 USD Received 9 Jan 2015; revised 16 Feb 2015; accepted 17 Feb 2015; published 5 Mar 2015

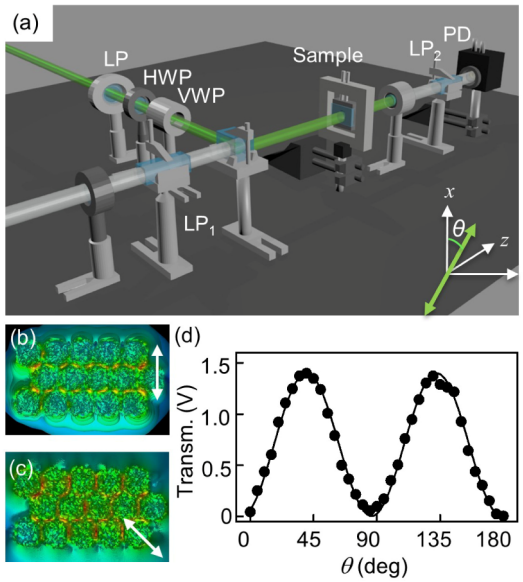

Fig. 5. (a) Optical set-up for rotating incident ***E*** field polarization. LP: linear polarizer; HWP: Half wave plate; VWP: Variable wave plate; PD: photo-detector. LP_1 and LP_2 are linear polarizers for the test WL beam. Resonant excitation is incident o the sample along the z-axis and the sample is mounted in the x-y plane. Simulations showing the scattered ***E*** field from an array of 30 nm AuNPs when the excitation is incident along the z-axis and resonant with the plasmon absorption at (b) $\theta = 0°$ and (c) $\theta = -45°$ (d) Transmission intensity with changing ***E*** polarization θ.

The dipole-like behavior of metallic NPs under plasmonic excitation implies that the ensemble has the usual anisotropic pattern of the near-field electric field commonly associated with dipole scattering and this directionality is determined by the incident exciting field. Figures 5(b) and 5(c) are simulated near-field intensity patterns for two different directions of linear polarization of the incident optical excitation at $\lambda = 532$ nm, as shown by the double-headed white arrows. Following the coordinates in Fig. 5(a), $\theta = 0°$ excitation creates hot spots only in the vertical interstitial regions but when the polarization is rotated by 45° there are highly localized high intensity regions in the lateral inter-particle gaps as well. The two cases must result in different orientation of the LC molecules in the plane of the sample, and we leverage this effect to control the in-plane LC directionality in addition to switching from homeotropic to planar. Figure 5(a) is a schematic of the optical set-up designed to continuously vary the linear polarization of the resonant excitation. Incident along the z-axis, the pump light first passes through a linear polarizer (LP) followed by a half wave plate (HWP) and a liquid crystal variable wave plate (VWP). These last two polarization optics allow us to continuously vary the angle of the linear polarization of light passing through them by externally controlling the birefringence of the VWP. The transmission intensity detected by the photo-detector (PD) beyond the sample is that of WL that passes through two crossed-polarizers (LP_1 and LP_2, aligned along $\theta = 0°$ and 90°), in the same arrangement as all previous measurements. Figure 5(d) shows this transmission voltage as a function of the incident polarization angle θ. The variation pattern indicates the in-plane LC orientation tracks the incident polarization exactly, showing no transmission when the polarization is along the optical axis of either polarizers, and maximum transmission when $\theta = 45°$ and 135°. This is a demonstration of a new all-optical in-plane switching mode where molecular orientation can be varied continuously, and faster than the out-of-plane switching [23]. The last question that remains is estimating the magnitude of the electric field generated in the near-field of AuNPs. We calculate our incident electric field to be 5 mV/μm, which, subject to

#232186 - $15.00 USD Received 9 Jan 2015; revised 16 Feb 2015; accepted 17 Feb 2015; published 5 Mar 2015

the enhancement factors, produces fields in the range 0.05 – 0.25 V/μm. These values are within the order of magnitude of threshold fields for switching of 5CB molecules in the nematic phase, and aided by localized thermal fluctuations on-resonance, is sufficient to cause the switching.

We have demonstrated a protocol to switch nematic LC molecules from homeotropic to planar by optical means alone, using near-field amplification of the electric field of excitation lying in the spectral band of the LPR of 30 nm AuNPs. This effect is macroscopic and completely reversible when the incident excitation is removed. Further, we have demonstrated that we can direct the in-plane orientation of the LC molecules as well, by modulating the incident polarization. The switching times associated with the re-orientation of LC molecules can be improved upon by either optimizing LC material and film thickness or by altering the morphology and sizes or the AuNPs to generate directional and stronger fields. Our findings offer a novel way to develop LC based devices with reduced ohmic losses by removal of electrical hardware and spectrally-selective response that opens the doors for entirely novel applications. In addition, by varying the type, shape and size of metallic NPs used, the bandwidth of spectral response could be modified from the visible to cover ultraviolet or near infra-red, allowing the development of optically-activated infra-red sensors and filters.

Acknowledgments

This work was supported by funds from UC Merced Graduate Research Council, and by awards from the National Science Foundation DMR-1056860 and in part by the NSF nanoBIO node, ECC-1227034.

#232186 - $15.00 USD Received 9 Jan 2015; revised 16 Feb 2015; accepted 17 Feb 2015; published 5 Mar 2015